Developing a Full Body Finite Element Model and Its Preliminary Validation for Seating Comfort

Shenghui Liu[1,2], Philippe Beillas[2,3], Li Ding[1], and Xuguang Wang[2,3]

[1] *Beihang University, China*

[2] *Université Gustave Eiffel-LBMC, France*

[3] *Université Claude Bernard Lyon 1, France*

Abstract

Human body finite element (FE) models can be used for seating comfort assessment by providing biomechanical related parameters such as internal loads and soft-tissue deformations. However, most of the published models were only validated under a condition far from a real seating situation. Their ability to be repositioned may also be limited. In recent years, an open-source PIPER software package has been developed to help personalize and position Human Body Models (HBMs) for crash simulation. We have morphed the PIPER Child model into an adult FE model. In this paper, we present how the initially morphed adult FE model was adapted for assessing seating comfort and validated for different seating conditions. Experimental data was collected using a reconfigurable experimental seat and pressure mats. Four seat configurations were defined with the seat pan angle (SPA) from 0° to 15° (5° in steps) and seat pan to seat backrest angle (SP2BA) kept to 100°. Simulated results in terms of seat contact area (ContactA), peak pressure (PeakP), mean pressure (MeanP), and pressure profiles showed good agreement with experimental observations. The full-body FE model developed and validated in this work will be used as a reference for further development of scalable and positionable models using the PIPER software framework. The model will be open source to facilitate reuse and further improvements.

Keywords: Seating dis/comfort, Full-body finite element model, Open-source, Validation

Introduction

People spend more and more time in a seating posture for transportation, office work, or leisure (Le and Marras, 2016). Improving seating comfort is not only a sale argument for seat manufacturers (Grujicic et al., 2009) but also important for consumers and healthcare-related fields (Oomens et al., 2015). Sustained loads on the soft tissue of the buttocks may cause seating discomfort or even physiological problems (Elsner & Gefen, 2008), especially for drivers and wheel-chair users (Cheng et al., 2018). However, soft tissue deformations and internal loading in terms of strain, and stress, which are generally considered relevant for seating discomfort assessment, cannot be all directly measured in vivo (De Looze et al., 2003).

With the development of computational capability, more and more researches have been devoted to build Finite Element (FE) HBM for assessing seating discomfort (Du et al., 2013; Levy et al., 2014). However, most of these models were not validated under real seating conditions including several postures, thus limiting their application to real world. For example, Al-Dirini et al. (2016) validated the model using only a rigid seat pan without a soft cushion. Huang et al. (2015) and Du et al. (2013) validated their models with a real seat under only one seat configuration. However, more seating conditions are needed for validating their sensitivity to seat parameter changes for seat comfort assessment.

In recent years, an open-source software package has been developed to personalize and position HBMs for crash simulation (available at www-piper-project.org). We also recently described the ongoing development of a full body adult FE model, morphed from the PIPER Child model (Liu et al., 2020). In this paper, we present how the initially morphed model was further adapted for assessing seating comfort at first, and then the preliminary validation results using the experimental data collected from a reconfigurable seat.

Model development

Developing a full-body finite element model is a time-consuming and complex process. Therefore, an open-source model, the PIPER Child model for impact simulation, was morphed into an adult-sized model. The baseline model corresponds to a 6 years old child, 1146 mm in stature. It includes 353 parts (deformable skull, brain, abdomen muscles, internal organs, neck, neck muscles, and pelvis, etc.) for a total of 531000 elements. The model was validated under multiple conditions for traffic injury assessment such as side-impact, and regional part validation including head, femur, neck, etc.(Beillas et al., 2016).

Brief description of the initial morphing

As presented in (Liu et al., 2020), we morphed the PIPER child model into an adult male. The morphing target was a male aged 40 years, 1740 mm in stature and 77.6 kg in weight. The morphing was based on different types of data collected on the same person. The spine and pelvis were obtained from the 3D reconstructions of the target subject who participated in a MRI study corresponding to a seated position with seat pan to backrest angle of 100° (Beillas et al., 2009). The same seating condition was reproduced for scanning the external body shape with a handheld laser scanner. After building the geometrical targets, the model was morphed by kriging interpolation using the PIPER software. The geometric errors and the elements quality were checked, and the model was used as the basis for further work.

Model adaptation

Numerous changes were carried out on the morphed model to adapt it to the comfort application. The main objectives were to (1) symmetrize it (2) reduce its computational cost (3) refine the mesh in regions of interest for seating comfort (4) adapt its material properties, which were initially selected for high-speed impact.

The work was initiated by symmetrizing the model with respect to the sagittal plane. The PIPER child model geometry and mesh are mostly symmetric. The exceptions are (1) the internal organs, which are not expected to be symmetric and will not be symmetrized, and (2) the mesh of some vertebrae and of the sternoclavicular ligaments, which will be symmetrized. Furthermore, the target geometry was directly derived from experimental data and hence, the geometry of the morphed model is not symmetric.

The vertebral meshes from the 12th thoracic vertebra (T12) to the 5th lumbar vertebra (L5) were first symmetrized within the PIPER child model (including intervertebral discs). For this, one side of the vertebral mesh was kept. This half side was used to generate solid elements before symmetrizing it (Figure 1 a and b). The sternoclavicular ligaments were also symmetrized by keeping one of the two sides.

Then, as the morphed model uses the same numbering scheme as the child model, the mesh symmetry of the child model were used to symmetrize the morphed model. First, the pairs of nodes that are symmetric with respect to the midsagittal plane and nodes laying on the midsagittal plane were identified in the child model. This allowed computing symmetric positions of these nodes on the morphed model by averaging (e.g. skeletal symmetry). However, this cannot be directly applied to the model as this approach would not transform the non-symmetric structures (e.g. internal organs). Hence, the symmetrized nodes were used as control points to transform the model using the Kriging in PIPER.
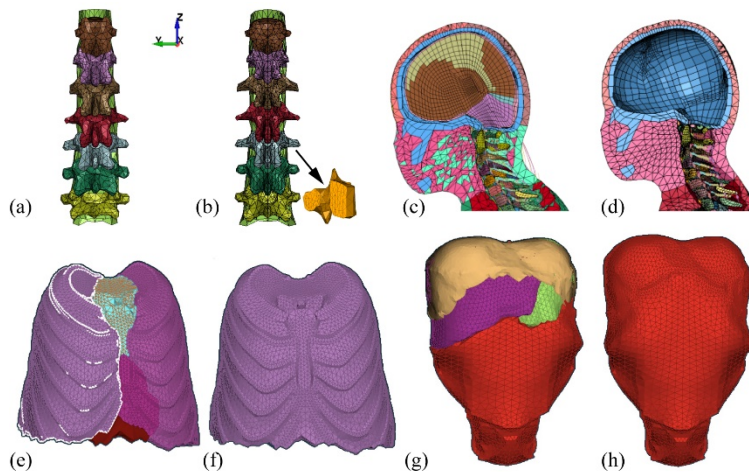
Figure 1 Comparison of some body structures before and after adaptation: lumbar vertebrae and intervertebral disc before and after symmetrisation (a,b), brain and neck muscles before and after simplifications (c,d), chest before and after simplification (e,f), abodomen before and after simplification (g,h)

The computational cost was then addressed. Some anatomical components which are marginally relevant for seating comfort were deleted, including the brain (initially modeled using hexahedral elements) and neck muscles (Figure 1 c and d). The mass of the brain was compensated for by increasing the skull density. The internal organs were also simplified into two incompressible controlled volumes described by their envelope (similar to airbags): one for the chest (Figure 1 e and f), and one for the abdomen organs (Figure 1 g and h). The mass of the organs was evenly distributed onto the nodes of the envelopes. The properties of the bones were changed to rigid (one rigid body per bone).

The buttock region was then refined as the simulation of the body and seat interaction in the region of the buttocks and thighs is of importance for seating comfort assessment. As shown in Figure 2a, the coccyx of the initial child model appears shorter than the one of adults, likely due to the presence of growth cartilage in that region (as the coccyx is not fully ossified at 6 years old, it could not be segmented on the CT scan). As the coccyx is an important anatomical structure that is susceptible to be involved in pressure ulcer (Farshbaf et al., 2013), the coccyx was modified based on adult data. As the pelvic skeleton derived from the MRI was in a low resolution, a pelvic segmentation from an adult CT-scan that is a publicly available (subject LTE605 available on www.piper-project.org) was scaled and aligned onto the pelvis model (Figure 2b) and used as a reference to adjust for the structure of the coccyx (Figure 2c).
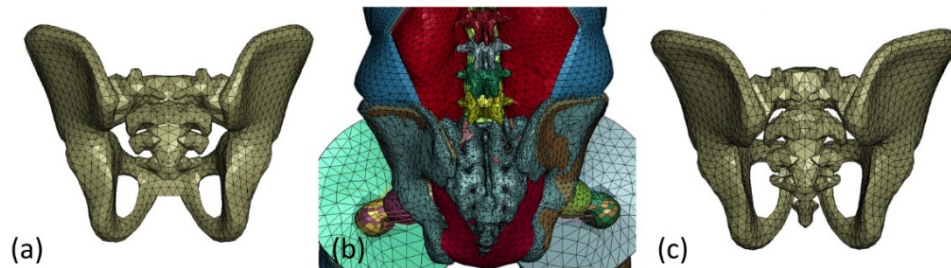

Figure 2 Replacement of the initial child coccyx by an adult one: the initially morphed pelvis based on the PIPER Child model (a), aligning an adult pelvis onto the model (b) and modified pelvis with an adult coccyx (c).

Then, as depicted in Figure 3, the mesh of the soft tissue underneath the ischial tuberosity (IT) was locally refined. This area is important for seating comfort assessments since it is the place with the highest pressure and a high risk of pressure ulcers (Tang et al., 2010) with a compressive strain of more than 50% (Elsner & Gefen, 2008; Sonenblum et al., 2013).
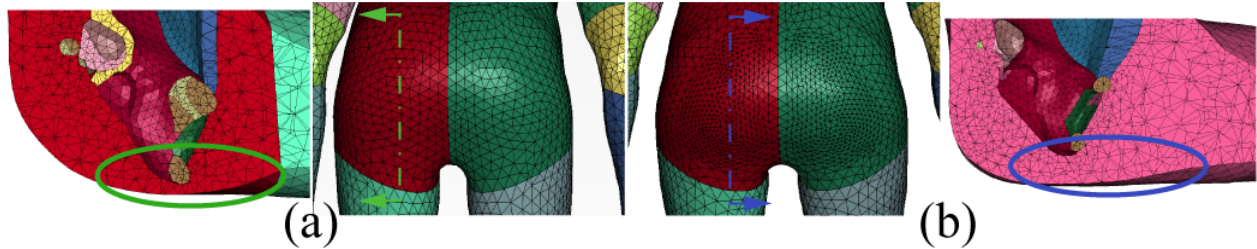
Figure 3 Local refinement of the soft tissue mesh under the ITs (a) mesh of the child model(b) refinement of the local mesh of buttocks with the adult model.

The geometry of the buttocks was obtained by the subject in a kneeling posture using a laser scan. It was not the same as the pre-sitting posture. The thickness of tissue was modified referring to the pre-loading seated MRI data from a study by (Wang et al., 2021). The shape of the buttocks before and after modification are shown in Figure 4. The soft tissue-ischium initial distance was set to 40mm.
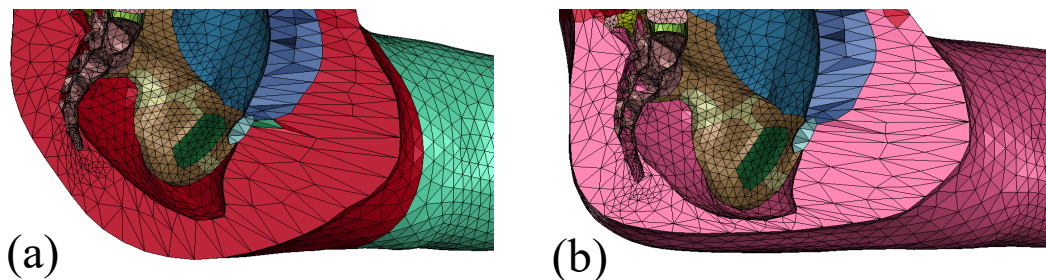

Figure 4 Buttocks shape. (a) the initial model using the kneeling posture obtained buttocks geometry. (b) pre-shaped after adaptation

The soft tissue material model and properties were changed from a simplified rubber to low modulus Neo Hookean model as in the work of Janak (2020) on obese modeling. The mass distribution of the model was checked and aligned with those by Huang et al. (2015) through adjusting the density of soft tissue and bone. The mass proportions are now 7.41%, 16.15%, 51.53%, 4.38% for the head, the lower limbs (thigh, calf, and foot), the torso, and the upper limbs (upper arm, forearm, and hands), respectively. Finally, some small penetrations and negative volume elements were fixed manually.

Model validation

Experimental data collection

To validate the model, an experiment was carried out with a reconfigurable experimental seat (Beurier et al., 2017). The participant was the person whose external scans and internal skeleton information were used as targets for the model development (Liu et al., 2020). Two wooden flat rectangular plates covered by a

foam of 50 mm thick were used for the seat pan (620 by 565 mm) and the seat backrest (550 by 550 mm). To measure the contact pressure, two sensor mats (XSENSOR, X3 PRO V6, Canada) were attached to the foam. Four configurations were tested varying the seat pan angle (SPA) from 0° (horizontal) to 15° in a step of 5°, while the seat pan to backrest angle (SP2BA) was fixed at 100° (Figure 5) corresponding to the seating configuration used in the MRI study by Beillas et al (2009). For each configuration, the participant was allowed to adjust the seat pan length and the foot support height to be seated comfortably. The subject was instructed to half flex his knees and the popliteal to the frontal seat edge was about 40mm.
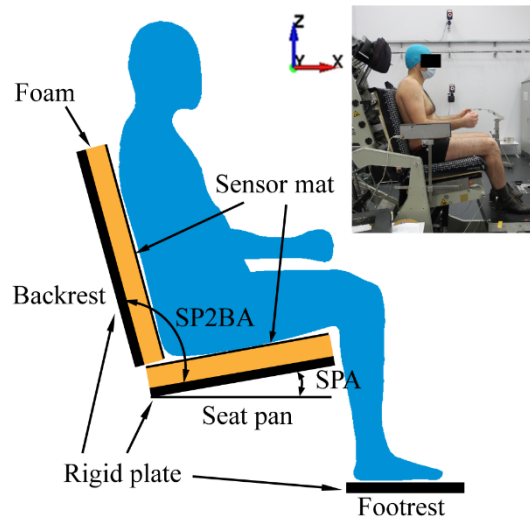

Figure 5. Experimental seat.

FE Simulation

The four experimental seating conditions were simulated with the developed adult model using LS-DYNA R11 MPP solver using 64 cores of a cluster. The time step was 2µs. Relaxation was used to help stabilize the contact force. The results (pressure, forces, etc.) were gathered at 400ms of simulation time, which took about 6 hours of elapsed time on the machines used for each simulation.

FE model prepositioning and boundary conditions

The bottom of the seat pan and backrest were fixed. The FE model was pre-positioned so that the back, buttocks and thighs were as close as possible to the seat without getting into contact. The feet were put on the footrest, which was simulated as a massless rigid body. To better control the distribution of the contact forces on the backrest, seat pan and footrest, the actual contact force on the footrest measured experimentally was imposed. For this, the footrest was oriented so that its normal direction was the same as the contact force measured experimentally. It was allowed to move only in this direction.

Automatic surface to surface contact was defined for the backrest and seat pan with a coefficient of friction (COF) of 0.1 (covered with the sensor map), while a COF of 0.4 was used for the footrest contact (Derler et al., 2008). To reduce computational time and maintain posture, we constrained some bones into one rigid body so that no relative movements were allowed between them: the skull and cervical spine, the calf and foot (left and right), the upper limb bones including the humerus, radius, ulna, hand (right and left bones). A gravity loading environment was applied.

To obtain the property of the foams on the seat pan and backrest, strain-stress curves were obtained through compression tests with a sample size of 8×8×5 cm using an Instron material testing machine. The curves are provided in the appendix.

Data analyses

Pressure and contact forces were compared between simulations and experiments. Pressure-related parameters include contact area (ContactA), mean pressure (MeanP), peak pressure (PeakP), and frontal and lateral pressure profiles (summation of pressure in rows and columns).

Results

Simulated and measured pressure distributions and profiles on the seat pan and backrest are compared in Figure 6 for the four test configurations. FE simulations were able to approach the corresponding measured pressure distributions (Figure 6a), with some discrepancies on the thighs and between the ITs. Some left/right asymmetry was visible in the experimental data, while the FE model responded symmetrically as expected. The differences were more pronounced for the backrest (Figure 6b), with some contacts near the pelvis which were not visible in the experiment. Predicted pressure profiles (Figure 6c) were close to the experimental data.
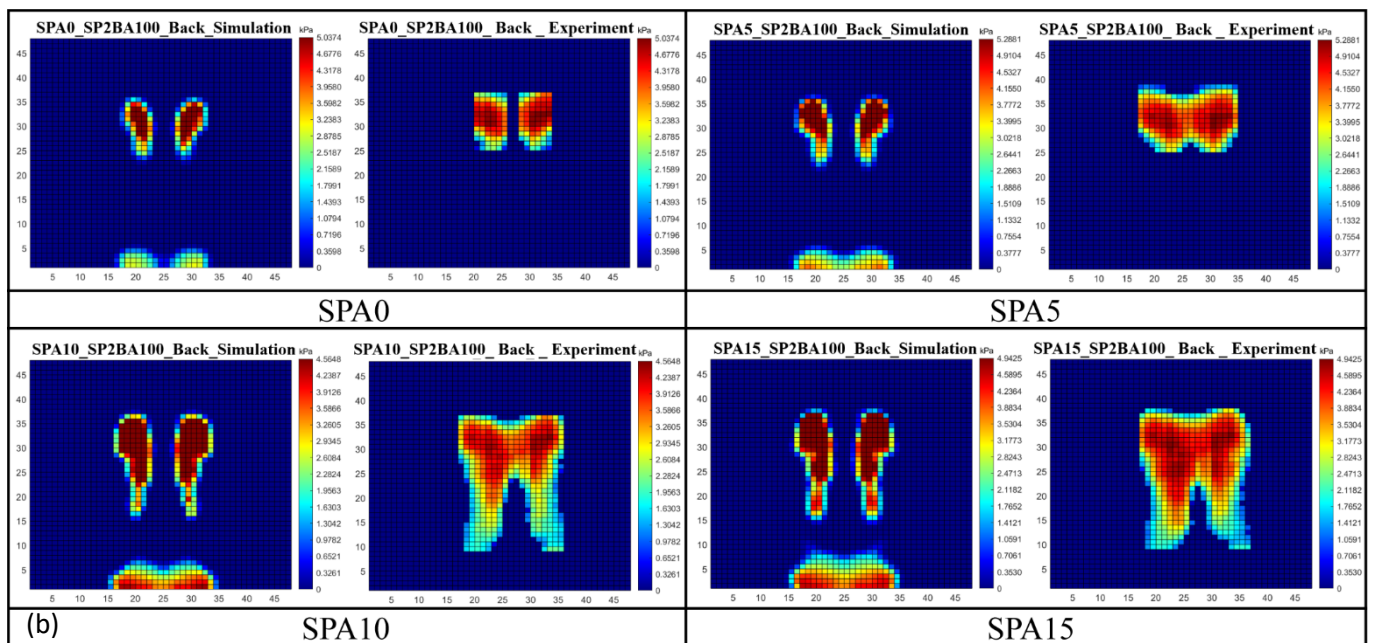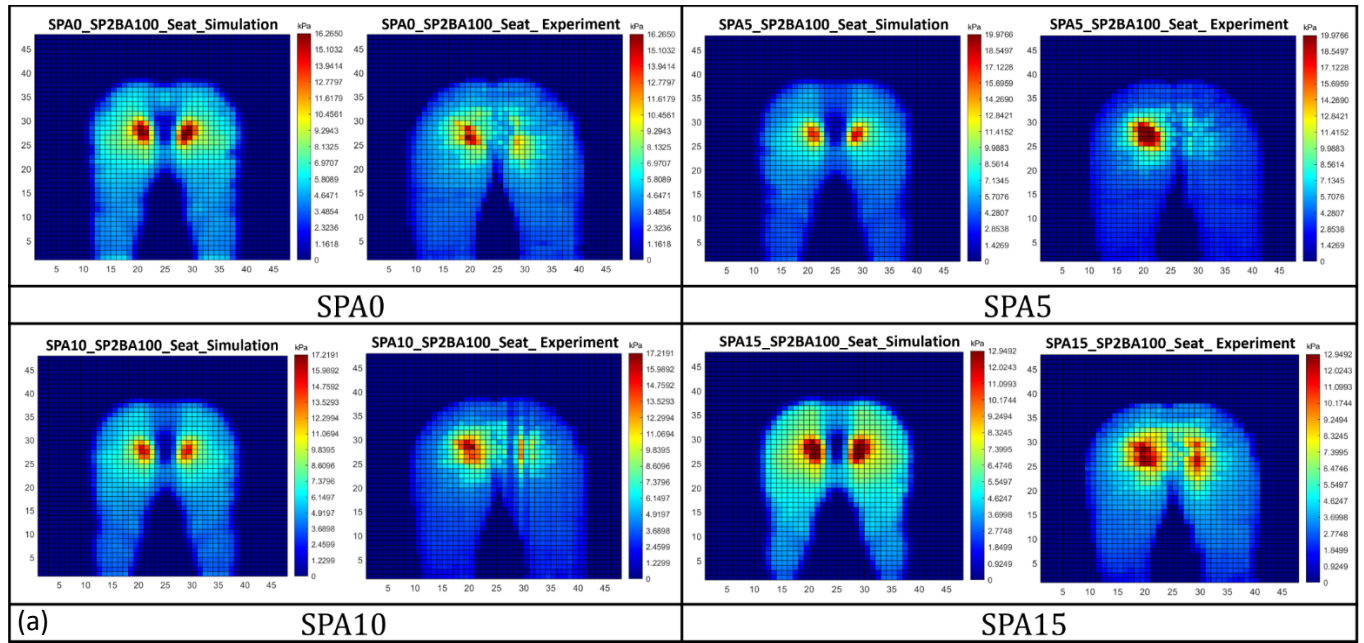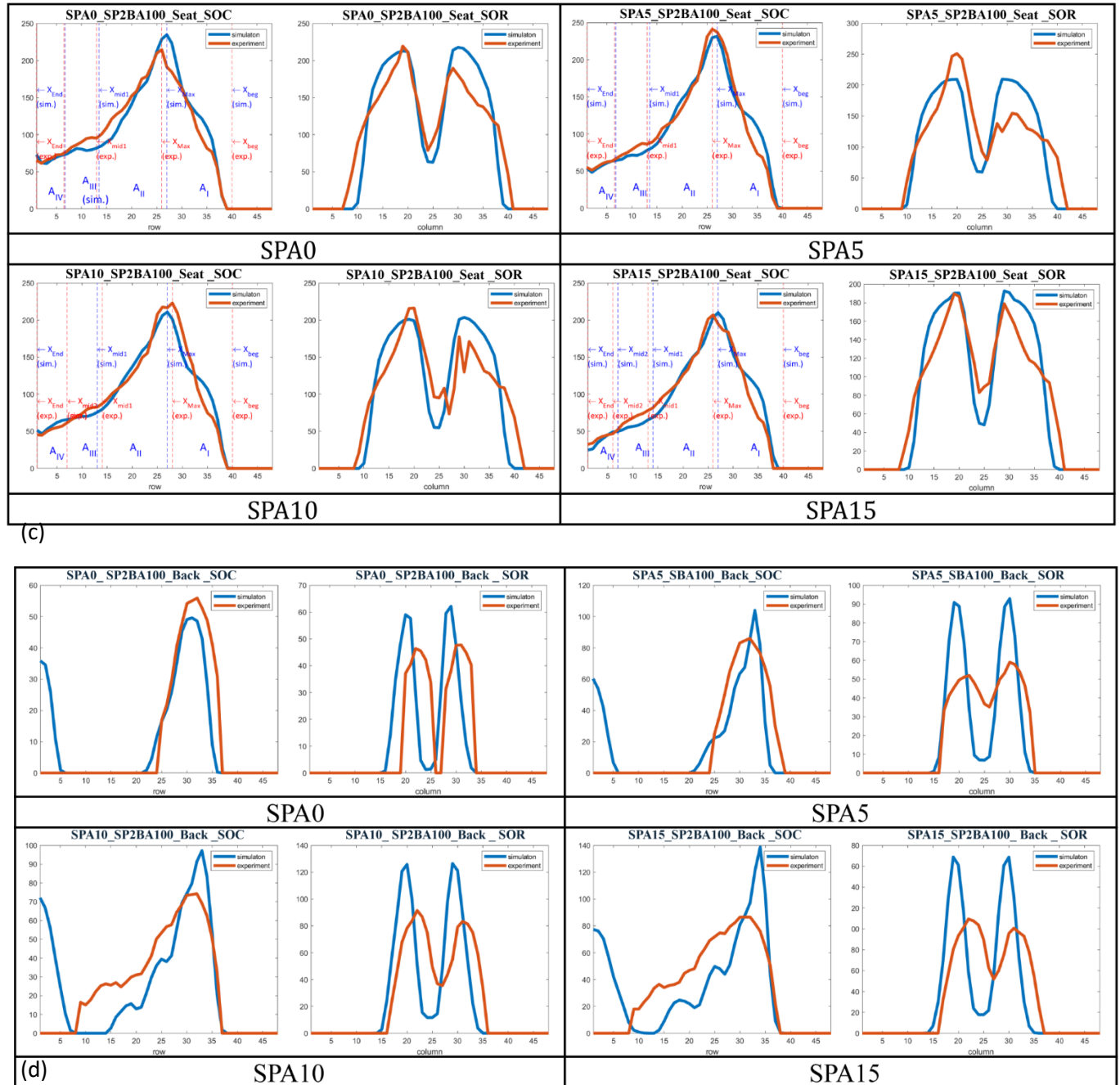
Figure 6. Comparison of simulated pressure distribution and profiles with experimental data for the four seat pan angles (SPA: 0°, 5°, 10° and 15°). (a) pressure on the seat pan, (b) pressure on the backrest, (c) lateral (SOC) and frontal (SOR) pressure profiles on the seat pan, (d) lateral (SOC) and frontal (SOR) pressure profiles on the backrest.

The contact area (ContactA); peak pressure (PeakP), mean pressure (MeanP), and shear (SF_SP) and normal (NF_SP) forces on the seat pan are summarized in Table 1. Compared to experimental data, the simulation had an average error of -3.2%, 3.8%, and 8.1% respectively for contact area, peak pressure, and mean pressure. Concerning contact force on the seat pan, simulated shear and normal forces showed the

same trend as experimental observations when increasing the seat pan angle. However, a high error in percentage was observed for shear force (up to 37.1%).

Table 1 Simulated (S) and experimental (E) values of contact area (ContactA), peak (PeakP), and mean pressures (MeanP), and contact forces: seat pan shear force (SF_SP), and normal force (NF_SP), as well as the errors (%) of simulation relative to experiment.

SPA (°)	ContactA (mm^2)		PeakP (kPa)			MeanP (kPa)			SF_SP (N)			NF_SP (N)		
	(S)	Error	(S)	(E)	Error	(S)	(E)	Error	(S)	(E)	Error	(S)	(E)	Error
0	162257.7	-4.0	16.8	16.3	3.4	4.6	4.3	8.7	58.7	59.2	-0.5	-709.0	-697.0	-12.0
5	161128.7	-2.6	17.4	20.0	-12.9	4.5	4.3	6.4	56.1	28	28.1	-689.5	-694.3	4.8
10	159031.9	-4.8	15.2	15.1	0.8	4.4	4.0	8.5	37.7	0.6	37.1	-661.6	-652.8	-8.8
15	153225.5	-3.7	15.4	12.4	23.9	4.2	3.9	8.7	31.8	-4.2	36.0	-607.9	-597.4	-10.5
Mean	158911.0	-3.2	16.2	15.9	3.8	4.6	4.1	8.1	46.1	20.9	25.2	-667.0	-660.4	-6.6
SD	3480.6	0.8	0.9	2.7	13.2	0.1	0.2	1.0	11.55	25.3	15.2	38.0	40.4	6.7

Discussion and Conclusions

Compared to experimental observations, simulated pressure distribution showed good agreement. Although the model did not simulate muscle forces, the targeted postures correspond to a relaxed state in which the muscle forces were expected to be small. The passive stiffness of the model and the choice of initial conditions hence played a role in the response. For example, there could be no contact near the pelvis on the backrest if the pelvis was positioned further away from the backrest. Overall, the choice of passive properties and boundary conditions appeared reasonable for the relaxed seating with an SP2BA of about 100°. They may need to be adjusted for postures that would further differ from the validation conditions (e.g. more reclined seating).

According to Figure 6, the simulated backrest pressure distribution and profiles had some differences compared to the experiment, especially in the lower back area and near the location of the scapulae. In simulations, the lower back was in contact with the backrest, while this was not the case for the experiment. This could be because the final loaded spine curvature was used at the preloading and the body may move under gravity: In addition, the initially scanned back shape is certainly not the same as the one that the subject adopted.

For the seat pan, the simulated contact areas (ContactA) were slightly smaller than the experimental results while the mean pressures (MeanP) were higher. As we can see from Figure 6, the middle area of between the two buttocks showed no contact in the simulation, quite different from experimental observations. Soft tissues were modeled a homogeneous material assuming an initial no strain / no stress state. More detailed

modeling of this area may be useful, including muscles and fat tissues. Most importantly, their initial strain states should be considered, as the body shape prior to loading is not known.

In this preliminary validation, only four configurations were tested with a fixed seat pan to backrest angle of 100°. Therefore, more seat configurations are needed to test the effect of seat parameters. Since the compression of the soft tissue under the ischial tuberosities is an important factor to evaluate seating comfort, the model will be further validated with soft tissue compressive deformations and observed using an open MRI (Wang et al., 2021).

In a summary, a personalized model for seating comfort has been developed and its predictions in terms of force and contact pressure distribution were checked against experimental data in four seat conditions. The models showed a reasonable agreement and further work will be conducted to expand upon the validation with more seating conditions and the analysis of local tissue deformation. The FE model will be published under an open source license to facilitate its reuse and improvement.

Acknowledgments

References

Al-Dirini, R. M. A., Reed, M. P., Hu, J., & Thewlis, D. (2016). Development and Validation of a High Anatomical Fidelity FE Model for the Buttock and Thigh of a Seated Individual. *Annals of Biomedical Engineering*, *44*(9), 2805–2816. https://doi.org/10.1007/s10439-016-1560-3

Beillas, P., Giordano, C., Alvarez, V. S., Li, X., Ying, X., Kirscht, S., & Kleiven, S. (2016). Development and Performance of the PIPER Scalable Child Human Body Models. *14th International Conference Protection of Children in Cars. Dec 8-9, 2016, Munich, Germany*, 1–19.

Beillas, P., Lafon, Y., & Smith, F. W. (2009). The effects of posture and subject-to-subject variations on the position, shape and volume of abdominal and thoracic organs. *Stapp Car Crash Journal*, *53*(November), 127–154.

Beurier, G., Cardoso, M., & Wang, X. (2017). A new multi-adjustable experimental seat for investigating biomechanical factors of sitting discomfort (No. 2017-01-1393). SAE Technical Paper.

Cheng, Z., Smith, J. A., Pellettiere, J. A., & Fleming, S. M. (2007). Considerations and experiences in developing an fe buttock model for seating comfort analysis (No. 2007-01-2458). SAE Technical

Paper.

De Looze, M. P., KUIJT-EVERS, L. F. M., & VAN DIEËN, J. (2003). Sitting comfort and discomfort and the relationships with objective measures. *Ergonomics*, *46*(10), 985–997. https://doi.org/10.1080/0014013031000121977

Derler, S., Kausch, F., & Huber, R. (2008). Analysis of factors influencing the friction coefficients of shoe sole materials. Safety Science, 46(5), 822–832. https://doi.org/10.1016/j.ssci.2007.01.010

Janák, T. (2020). Personalization of human body models to simulate obese occupants in automotive safety .(pp.140) ,Université Claude Bernard - LYON 1, Lyon , France.

Du, X., Ren, J., Sang, C., & Li, L. (2013). Simulation of the interaction between driver and seat. *Chinese Journal of Mechanical Engineering*, *26*(6), 1234–1242. https://doi.org/10.3901/cjme.2013.06.1234

Elsner, J. J., & Gefen, A. (2008). Is obesity a risk factor for deep tissue injury in patients with spinal cord injury? *Journal of Biomechanics*, *41*(16), 3322–3331. https://doi.org/10.1016/j.jbiomech.2008.09.036

Farshbaf, M., Yousefi, R., Pouyan, M. B., Ostadabbas, S., Nourani, M., & Pompeo, M. (2013). Detecting high-risk regions for pressure ulcer risk assessment. In 2013 IEEE International Conference on Bioinformatics and Biomedicine (pp. 255-260). IEEE.

Grujicic, M., Pandurangan, B., Arakere, G., Bell, W. C., He, T., & Xie, X. (2009). Seat-cushion and soft-tissue material modeling and a finite element investigation of the seating comfort for passenger-vehicle occupants. *Materials and Design*, *30*(10), 4273–4285. https://doi.org/10.1016/j.matdes.2009.04.028

Huang, S., Zhang, Z., Xu, Z., & He, Y. (2015). Modeling of human model for static pressure distribution prediction. International Journal of Industrial Ergonomics, 50, 186-195.. https://doi.org/10.1016/j.ergon.2015.09.017

Le, P., & Marras, W. S. (2016). Evaluating the low back biomechanics of three different office workstations: Seated, standing, and perching. *Applied Ergonomics*, *56*, 170–178. https://doi.org/10.1016/j.apergo.2016.04.001

Levy, A., Kopplin, K., & Gefen, A. (2014). An air-cell-based cushion for pressure ulcer protection remarkably reduces tissue stresses in the seated buttocks with respect to foams : Finite element studies. *Journal of Tissue Viability*, *23*(1), 13–23. https://doi.org/10.1016/j.jtv.2013.12.005

Liu, S., Beillas, P., Ding, L., & Wang, X. (2020). Morphing an existing open source human body model into a personalized model for seating discomfort investigation. SAE Int, 2020, 01-0874

Oomens, C. W. J., Bader, D. L., Loerakker, S., & Baaijens, F. (2015). Pressure Induced Deep Tissue Injury Explained. *Annals of Biomedical Engineering*, *43*(2), 297–305. https://doi.org/10.1007/s10439-014-1202-6

Bader, D. L., Bouten, C., Colin, D., & Oomens, C. W. (Eds.). (2005). Pressure ulcer research: current and future perspectives., pp.150-155.

Sonenblum, S. E., Sprigle, S. H., Cathcart, J. M. K., & Winder, R. J. (2013). 3-dimensional buttocks response to sitting: A case report. *Journal of Tissue Viability*, *22*(1), 12–18. https://doi.org/10.1016/j.jtv.2012.11.001

Tang, C. Y., Chan, W., & Tsui, C. P. (2010). Finite Element Analysis of Contact Pressures between Seat Cushion and Human Buttock-Thigh Tissue. *Engineering*, *02*(09), 720–726. https://doi.org/10.4236/eng.2010.29093

Wang, X., Savonnet, L., & Duprey, S. (2021). A Preliminary Study on the Effects of Foam and Seat Pan Inclination on the Deformation of the Seated Buttocks Using MRI. In Congress of the International Ergonomics Association (pp. 434-438). Springer, Cham.

Yadav, S. K., Huang, C., Mo, F., Li, J., Chen, J., & Xiao, Z. (2021). Analysis of seat cushion comfort by employing a finite element buttock model as a supplement to pressure measurement. *International Journal of Industrial Ergonomics*, *86*(May 2020), 103211. https://doi.org/10.1016/j.ergon.2021.103211

Appendix
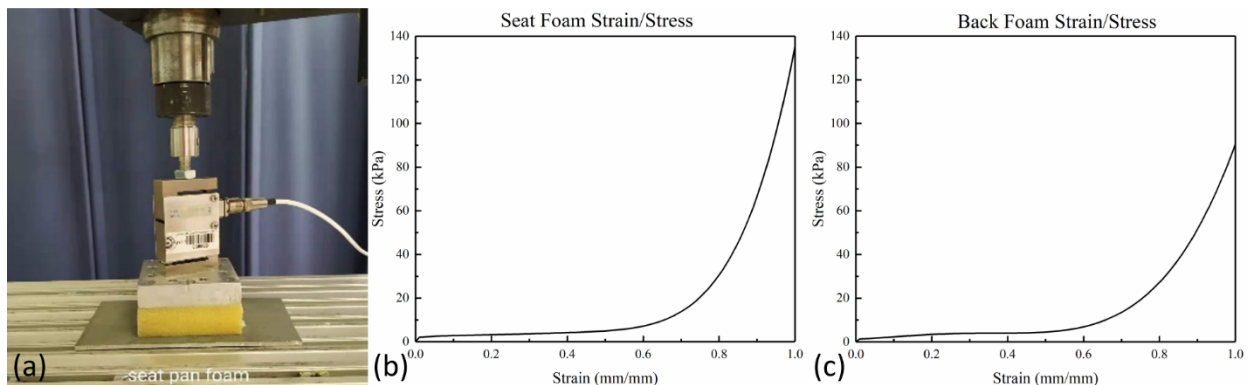
Seat pan and backrest foam strain-stress curves